Supporting Information

Ngodup et al. 10.1073/pnas.1420885112

SI Materials and Methods

Noise Exposure. CBA/CaJ mice of either sex (The Jackson Laboratory) were reared in constant broadband noise (1.6–39 kHz in frequency range) using a white noise generator (ACO Pacific 3025), driving a Fostex speaker (FT28D) mounted above the animal cage. The sound level was measured with a sound level meter (Larson–Davis 824) at the center of the cage, and ranged from 90 to 94 dB sound pressure level (SPL). Most mice were exposed to noise from P12 until electrophysiological brain slice recordings were performed after P18. In some mice, noise exposure was ended at P26.

Brain Slice Electrophysiology. Parasagittal slices of AVCN were cut from the auditory brainstem of P18–P62 CBA/CaJ mice as described previously (1). Briefly, animals were anesthetized and decapitated, and the brain was removed and placed into low-sodium, ice-cold cutting solution. We used two different cutting solutions. One was sucrose-based containing 76 mM NaCl, 26 mM $NaHCO_3$, 75 mM sucrose, 1.25 mM NaH_2PO_4, 2.5 mM KCl, 25 mM glucose, 7 mM $MgCl_2$, and 0.5 mM $CaCl_2$, bubbled with 95% O_2:5% CO_2 (pH 7.8, 305 mOsm). The other was standard recording solution containing 125 mM NaCl, 26 mM $NaHCO_3$, 1.25 mM NaH_2PO_4, 2.5 mM KCl, 20 mM glucose, 1 mM $MgCl_2$, 1.5 mM $CaCl_2$, 4 mM Na L-lactate, 2 mM Na-pyruvate, and 0.4 mM Na L-ascorbate, bubbled with 95% O_2:5% CO_2 (pH 7.4, 310 mOsm). Slices were cut at a slight angle from sagittal, to best preserve straight projections of the AN. Slices were cut at 150 μm thickness and incubated at 32 °C for 15–20 min in a recovery solution containing 93 mM NMDG, 93 mM HCl, 2.5 mM KCl, 1.2 mM NaH_2PO_4, 30 mM $NaHCO_3$, 20 mM Hepes, 25 mM glucose, 5 mM Na ascorbate, 3 mM Na pyruvate, 10 mM $MgCl_2$, and 0.5 mM $CaCl_2$ and then transferred to standard recording solution. Slices were then maintained at room temperature until recording.

Slices were viewed using an Olympus BX51WI microscope with a 60× objective. Whole cell patch-clamp recordings were made from BCs using an Axopatch 700B amplifier (Molecular Devices) at 34 °C in the presence of 10 μM strychnine. Recording electrodes contained, for voltage clamp, 35 mM CsF, 100 mM CsCl, 10 mM EGTA, 10 mM Hepes, and 1 mM *N*-(2, 6-dimethylphenyl carbamoylmethyl) triethylammonium chloride (QX-314) or, for current clamp, 130 mM $KMeSO_3$, 10 mM NaCl, 2 mM $MgCl_2$, 0.16 mM $CaCl_2$, 0.5 mM EGTA, 10 mM Hepes, 2 Na_2ATP, 0.4 mM NaGTP, and 14 mM Tris-CrPhos (pH 7.2, 302 mOsm).

Pipettes were pulled from 1.5-mm OD, 0.86-mm ID borosilicate glass (Sutter Instrument) to a resistance of 1–2 MΩ. In voltage clamp, cells were held at −70 mV, with access resistance 5–15 MΩ compensated to 70%. In current clamp, resting potential was maintained at −60 mV between trials by passing up to ±300 pA. BCs were identified in voltage clamp by EPSC having rapid decay kinetics ($\tau < 0.2$ ms) and half-width ≤ 0.5 ms (2) and, in current clamp, by their response to strong depolarizing current pulses with 1–2 undershooting spikes (3). AN fibers were stimulated using a glass microelectrode placed 30–50 μm away from the soma (A365; WPI). Single or paired pulses were applied every 10 s. Train stimuli were applied every 30 s. Stimulation and data collection were done using a PCI-6221 (National Instruments) controlled using custom-written software (mafPC) running in Igor (WaveMetrics).

Morphology. To study the morphology of BCs for Fig. S1, recording pipette solution included 0.2% neurobiotin. After loading each cell, the recording electrode was retracted, and the slice was fixed overnight in 4% (wt/vol) buffered paraformaldehyde. To visualize neurobiotin, the slices were rinsed with PBS, sections were then incubated in ABC reagent (Vector Laboratories) for 2 h, rinsed with PBS, incubated for 3–4 min in 0.05% diaminobenzidine, 0.3% H_2O_2, and nickel chloride solution, mounted onto subbed slides, and coverslipped under Depex. Cells were reconstructed using a camera.

Immunohistochemistry. Mice were anesthetized with 200 mg/kg ketamine:10 mg/kg xylazine. Then perfused transcardially with 0.9% saline followed by 4% buffered paraformaldehyde. Brains were removed and postfixed for 2 h before cryoprotecting overnight in 20% (wt/vol) sucrose. Sagittal sections were cut frozen at 40 μm thickness on a sliding microtome (American Optical). Slices were treated with 0.5% Triton X-100 in 0.2 M PBS for 10 min. The slices were then blocked in 1% normal goat serum for 1 h at room temperature. The sections were incubated overnight at 4 °C in primary antibody solution containing: anti–VGLUT-1 (Invitrogen) at 1:500, 1% goat serum, and 0.2 M PBS with 0.1% Triton X-100. The sections were then washed three times in 0.2 M PBS solution and incubated for 2 h with 1:200 Texas-red–conjugated goat anti-rabbit antibody (Jackson ImmunoResearch Laboratories) in 0.2 M PBS, 0.1% Triton X-100, and 1% goat serum. The sections were then mounted on glass slides using Fluoromount G with DAPI (Southern Biotech). Images were acquired using a Zeiss Meta LSM 510 confocal microscope. All of the quantification of puncta was performed blind to rearing conditions. We quantified the cross-sectional area of puncta in the optical section taken at the midline of each cell. We drew around the puncta where the labeling was above the background. Images were analyzed using ImageJ.

Ribbon synapses at inner hair cells were analyzed for Fig. S3 using the approach described previously (4–6). Cochlea was perfused with 4% paraformaldehyde and postfixed 1–2 h. The organ of Corti was removed from the cochlea, and segments from apex, middle, and base were obtained. The segments were incubated overnight at 4 °C in primary antibody solution containing anti-CtBP2 (Biosciences) at 1:200, anti-calretinin (Sigma) at 1:1,000, 1% goat serum, and 0.2 M PBS with 0.1% Triton X-100. The segments were then washed three times in 0.2 M PBS solution and incubated for 2 h with 1:200 Texas-red–conjugated goat anti-rabbit antibody (Jackson ImmunoResearch Laboratories) and 1:200 Alexa Fluor 488 goat anti-mouse (Life Technologies) in 0.2 M PBS, 0.1% Triton X-100, and 1% goat serum. The segments were mounted on glass slides using Fluoromount G with DAPI (Southern Biotech). Images were acquired using a Zeiss Meta LSM 510 and Olympus Fluoview confocal microscope and analyzed using Olympus Fluoview Image browser and ImageJ.

Electron Microscopy. Brains were embedded in gelatin-albumin, and 75- to 100-μm sections were cut using a Vibratome. Sections were osmicated for 5–10 min, rinsed in maleate buffer, and stained with uranyl acetate. Sections were again rinsed in maleate buffer and dehydrated in graded alcohols. Residual ethanol was removed with propylene oxide, and the sections were infiltrated with Polybed 812. Sections were mounted flat between sheets of Aclar and hardened in a 60 °C oven. Pieces of flat sections containing BCs in the AVCN were excised and reembedded in Polybed 812 in BEEM capsules. Specimens were then sectioned at 60–75 nm and placed on mesh or formvar-coated slot grids. Ultrathin sections were stained with uranyl acetate and lead citrate to improve contrast. Random sections were scanned for BCs

with characteristics described (7) at low magnification (2,000–3000×) using a Hitachi H7600 transmission electron microscope. AN synapses with characteristic large round synaptic vesicles, clear cytoplasm, and identifiable postsynaptic densities were photographed at high magnification (25,000–30,000×). Axosomatic synapses were photographed. Electron micrographs of AN synapses were adjusted to produce similar brightness and contrast across all images. Ultrastructural features were traced by a blind observer using Adobe Photoshop software and a Wacom Cintiq interactive drawing tablet. Ultrastructural features were measured using ImageJ software.

Auditory Brainstem Responses. ABRs were assessed in noise-reared animals after returning them to normal sound conditions at P26, and allowing recovery of 2– 4 wk. Mice were anesthetized with a dose of 200 mg/kg ketamine:10 mg/kg xylazine. ABRs were recorded with a vertex electrode and an electrode inserted behind the pinna ipsilateral to the stimulated ear and the ground electrode inserted contralateral to the stimulated ear. Clicks of 100 μs duration were presented through a speaker placed into the external ear canal. ABR threshold was obtained for each animal by reducing the stimulus intensity in 10 dB steps and finally 5 dB steps to identify the lowest intensity at which an ABR wave III was detectable. ABR was recorded in a sound-proof room with BioSigRP software (TDT) and TDT hardware (8). The ABR peaks were identified following the nomenclature of refs. 9 and 10. Average results are reported throughout as mean ± SEM. Test of significance is usually reported as unpaired *t* test, unless otherwise mentioned.

1. Yang H, Xu-Friedman MA (2010) Developmental mechanisms for suppressing the effects of delayed release at the endbulb of Held. *J Neurosci* 30(34):11466–11475.
2. Chanda S, Xu-Friedman MA (2010) A low-affinity antagonist reveals saturation and desensitization in mature synapses in the auditory brain stem. *J Neurophysiol* 103(4): 1915–1926.
3. Oertel D (1983) Synaptic responses and electrical properties of cells in brain slices of the mouse anteroventral cochlear nucleus. *J Neurosci* 3(10):2043–2053.
4. Kujawa SG, Liberman MC (2009) Adding insult to injury: Cochlear nerve degeneration after "temporary" noise-induced hearing loss. *J Neurosci* 29(45):14077–14085.
5. Grant L, Yi E, Goutman JD, Glowatzki E (2011) Postsynaptic recordings at afferent dendrites contacting cochlear inner hair cells: Monitoring multivesicular release at a ribbon synapse. *J Vis Exp* 2011(48):2442.
6. Khimich D, et al. (2005) Hair cell synaptic ribbons are essential for synchronous auditory signalling. *Nature* 434(7035):889–894.
7. Lauer AM, Connelly CJ, Graham H, Ryugo DK (2013) Morphological characterization of bushy cells and their inputs in the laboratory mouse (Mus musculus) anteroventral cochlear nucleus. *PLoS ONE* 8(8):e73308.
8. Sun W, et al. (2009) Salicylate increases the gain of the central auditory system. *Neuroscience* 159(1):325–334.
9. Popescu MV, Polley DB (2010) Monaural deprivation disrupts development of binaural selectivity in auditory midbrain and cortex. *Neuron* 65(5):718–731.
10. Melcher JR, Kiang NY (1996) Generators of the brainstem auditory evoked potential in cat. III: Identified cell populations. *Hear Res* 93(1-2):52–71.

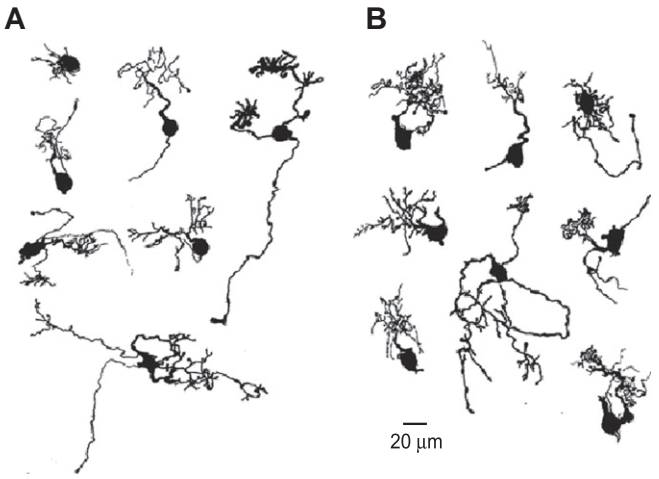

Fig. S1. Morphology of BCs. BCs from control and noise-reared mice were filled with neurobiotin to reconstruct their structure. BCs exhibited typical single axon and profusely branched dendrites in both (*A*) control (n = 12) and (*B*) noise-reared animals (n = 13).

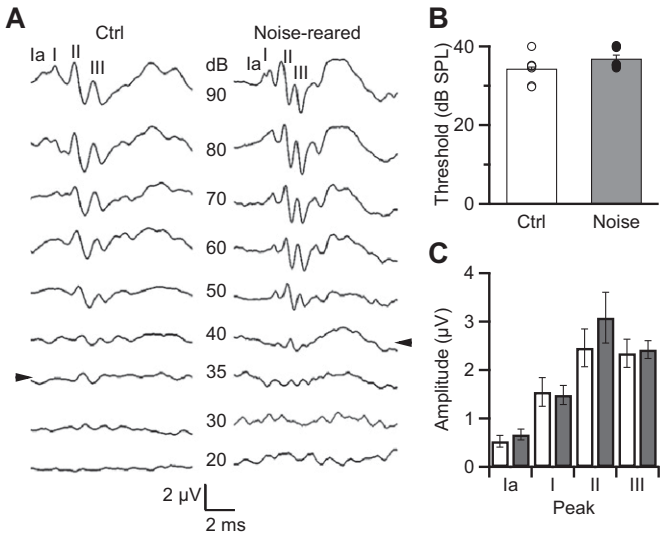

Fig. S2. Noise treatment does not cause permanent threshold shift in ABR. (*A*) Representative ABR traces from P49 control (*Left*) and noise-reared (*Right*) mice in response to click stimuli. Arrowheads indicate threshold for control and noise-reared animals. (*B*) The mean ABR threshold for control ($n = 3$) and noise-reared animals ($n = 4$). There was no significant difference ($P > 0.5$, *t* test). (*C*) ABR amplitudes of waves Ia, I, II, and III in response to 80-dB click stimuli. ABR amplitudes of noise-reared animals were not significantly different from the control animals ($P > 0.1$ for all).

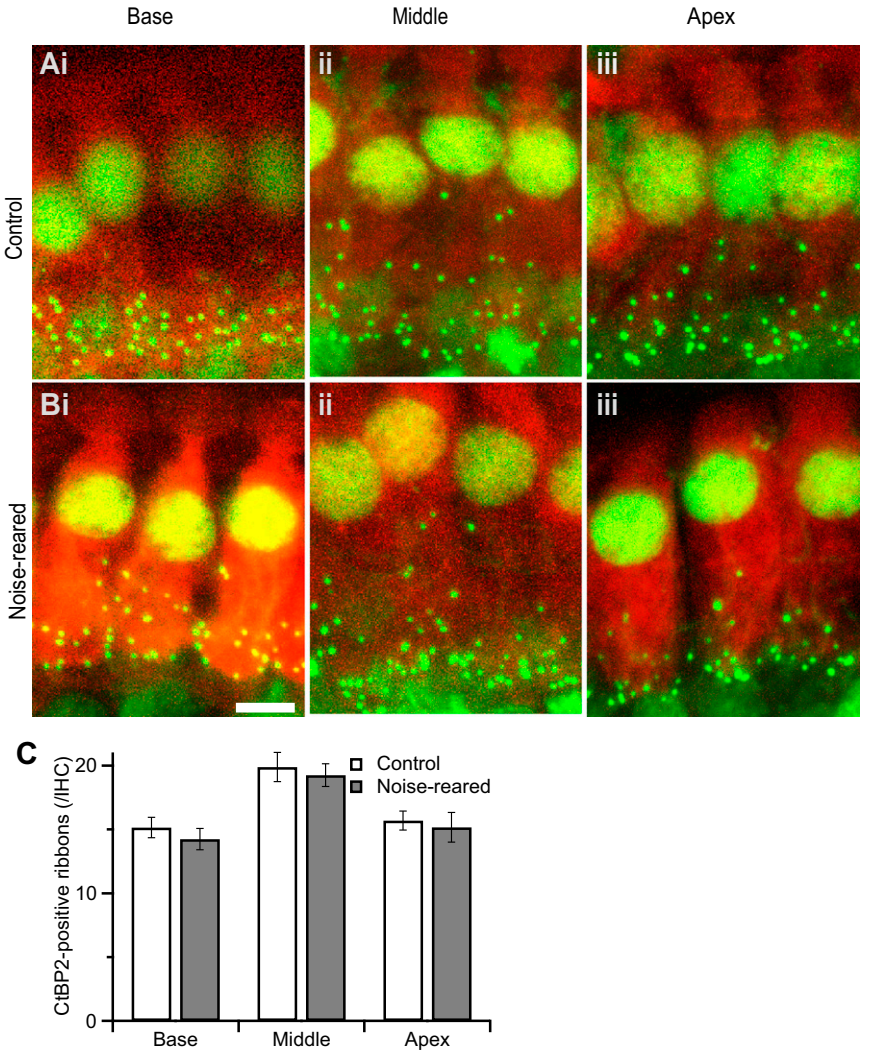

Fig. S3. Noise rearing does not show loss of synaptic ribbons at hair cell synapses. (*A* and *B*) Representative image of inner hair cell (red, anti-calretinin) showing ribbon synapses (green, anti-CtBP2) from three (*i*, base; *ii*, middle; and *iii*, apex) different cochlear region from control (*A*) and noise-reared (*B*) cochlea. (*C*) Synaptic ribbon counts from base, middle, and apex did not show any significant loss of ribbons and no obvious change in spatial distribution of ribbons in noise-reared cochleas (n = 14–21 cells in each region, $P > 0.4$). (Scale bar: 5 μm.)

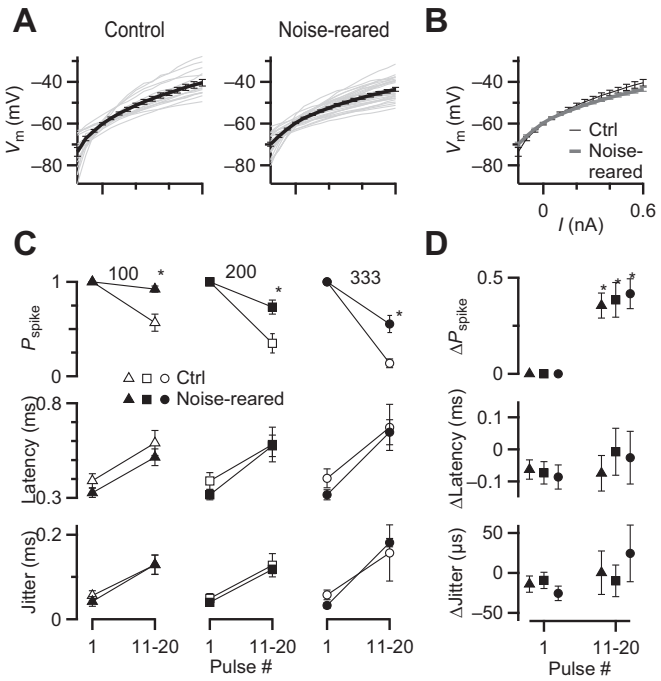

Fig. S4. Effects of noise rearing on spike generation and spiking probability in BCs. (*A* and *B*) No changes in input resistance after noise rearing. Shown are I-V curves for 15 control BCs (*A*, *Left*) and 30 BCs from noise-reared mice (*A*, *Right*). Dashed lines in *A* are measurements in individual cells, with averages shown in solid lines in *B*. (*C*) Average P_{spike}, spike latency, and spike jitter during fiber stimulation at 100, 200, and 333 Hz. Quantification was made of the first pulse in the train, and pulses 11–20. Asterisks mark significant changes ($P < 0.05$). (*D*) Relative changes in P_{spike} (*Top*), latency (*Middle*), and jitter (*Bottom*) for BCs from control and noise-reared animals.